WILEY-VCH

Edited by Vineet K. Rai

# Upconverting Nanoparticles

## From Fundamentals to Applications

**Upconverting Nanoparticles**

# Upconverting Nanoparticles

From Fundamentals to Applications

*Edited by Vineet K. Rai*

WILEY-VCH

**Editor**

***Prof. Dr. Vineet K. Rai***
IIT (ISM) Dhanbad
Department of Physics
Police Line Road
Hirapur, Sardar Patel Nagar
826004 Dhanbad
India

**Cover Image**:
© BAIVECTOR/Shutterstock



**Library of Congress Card No.:** applied for

**British Library Cataloguing-in-Publication Data**
A catalogue record for this book is available from the British Library.

**Bibliographic information published by the Deutsche Nationalbibliothek**
The Deutsche Nationalbibliothek lists this publication in the Deutsche Nationalbibliografie; detailed bibliographic data are available on the Internet at <http://dnb.d-nb.de>.



**Print ISBN:** 978-3-527-34965-4
**ePDF ISBN:** 978-3-527-83486-0
**ePub ISBN:** 978-3-527-83487-7
**oBook ISBN:** 978-3-527-83488-4

**Typesetting** Straive, Chennai, India

Printed on acid-free paper

10 9 8 7 6 5 4 3 2 1

# Contents

# Preface

The conversion of low-energy photons into high-energy photons, known as "frequency upconversion," using advanced optical materials has become an emerging research field with wide consequence and impact in various scientific areas ranging from healthcare to energy and security. The materials showing frequency upconversion properties are known as upconversion (UC) materials. UC materials reveal variety of applications in different fields, viz. color display, two-photon imaging in confocal microscopy, WLEDs, high-density optical data storage, upconvertors, under sea communications, solid-state lighting, sensors, photovoltaics, photocatalysis, food industry, indicators, anti-counterfeiting, bioimaging, cancer therapy and other biological fields. It is known that in comparison to ultraviolet (UV) and visible light the near-infrared (NIR) light is abundant and non-destructive in nature. It has deep penetration in the organisms and less harmful quality. UC luminescent materials in nanosize range are known as UC nanomaterials or UC nanoparticles (UCNPs). UCNPs excited with non-destructive NIR light are a better choice than the conventional downconversion nanoparticles because they are free from autofluorescence, have low light penetration, and cause less severe photo-damage to living organisms. It is notable to mention that the low efficiency of UC materials definitely becomes a major barrier for their application in a wide range. For researchers, it is a top priority to overcome this problem. Several engineered UCNPs, e.g. organic, inorganic, hybrids, and thin films, have been explored widely to obtain highly efficient UC luminescent materials. Usually, organic luminescent materials suffer poor stability under harsh conditions and have poor long-term reliability, but have a greater ductility than inorganic materials. The inorganic luminescent materials are more durable and possess high thermal stability. So, the hybrid materials consisting of both inorganic and organic components, namely, metal organic frameworks (MOFs), have attracted researchers with enhanced luminescence properties as compared to the bare organic and inorganic materials. To enhance the upconversion efficiency, spherical metal nanoparticles showing plasmon resonance in close proximity of the UCNPs are utilized. The plasmonic nanostructures are widely used to evolve the UCNPs with improved electronic, metallic, and optical properties. When the surface plasmon resonance wavelength of the metallic nanostructure matches with the excitation wavelength of upconversion mechanism, signal enhancement occurs. Usually, the coating of

gold (Au) and silver (Ag) nanoparticles is used to tune the luminescence properties of UCNPs, though the nanoparticles exhibit plasmon absorption in 400–600 nm range.

The upconversion emission efficiency can be enhanced by several ways, including doping with sensitizer, non-lanthanides, and coating with inorganic shell. The non-lanthanide co-doping in UCNPs has also been used frequently in order to get enhanced luminescence intensity along with the use of sensitizer ion. The co-doping of activator and sensitizer ions with proper concentration in an appropriate host matrix is essential to achieve highly efficient UC emission as the concentration quenching has a prejudicial effect on the luminescence intensity. The phonon frequency, stability, cost effectiveness, non-hygroscopic, and non-toxic nature of the UC materials are of utmost importance. The security of any important data, currency, etc. has become very crucial to prevent counterfeiting. UCNPs with high luminescence intensity can be validated in anti-counterfeiting applications. These materials are also utilized for visual exposure of fungicides, thiram, etc., which can be broadly applied in soybeans, apples, wine farming, etc., to avoid crop diseases and excessive use of pesticides. Rare-earth-ions-based UC emission has tremendous advantages in terms of long excited lifetime, sharp emission bandwidth, low autofluorescence, high photostability, high resolution, low toxicity, etc. Rare-earth ions are found to be very sensitive to even small changes in chemical surroundings. Therefore, it becomes essential to get information about the symmetry, bonding of the probe ion, and how they change their optical properties with chemical composition of the host materials. For getting the high quantum efficiency, concentration of the dopants should be high, but it may cause concentration quenching due to the interaction between the excited and unexcited neighbors. Therefore, the nano-structured materials containing metallic nanoparticles are of particular interest because the large local field around the rare-earth ions positioned near the nanoparticles may increase the luminescence efficiency. Among several strategies, the coating of upconversion nanoparticles with inorganic materials shell is an effective method to get enhanced UC luminescence. The core@shell approach offers shielding to the surface particles and thus reduces the surface defects and possibility of quenching. This core@shell architecture is very much beneficial in biomolecule conjugation and thus suitable for many biological applications. Different coating strategies have been employed according to the required application purposes. UCNPs probes can function as multiple contrast agents for concurrent use in altered medicinal imaging modalities by providing corresponding diagnostic information (i.e. MRI and CT). Bio-conjugation on the surface of the UCNPs shows a much enhanced imaging performance in comparison to the clinically used fluorescent dyes. Innovative bio-imaging methods are being established by combining the conventional medical imaging modalities using core-shell structured UCNPs.

The book entitled *Upconverting Nanoparticles: From Fundamentals to Applications* is completely different from the previously published books in all respects, including the basics, scientific and technological demands. It is divided into eighteen chapters. Chapter 1, authored by Mondal and Rai, introduces the basic

concepts of upconversion, and upconversion of nano-particles. The introduction to frequency upconversion and its various mechanisms, excitation and de-excitation processes in hosts containing rare-earth ions along with the spectroscopic properties of rare-earth ions/transition metals are described in this chapter. The rate equations relevant to excited-state absorption and energy transfer processes with an overview of the UCNPs have been introduced. Chapter 2, authored by Mukhopadhyay and Rai, describes the synthesis protocol of upconversion nanoparticles. In this chapter introduction to host materials and synthesis strategies of UC nanomaterials like solid-state reaction, co-precipitation, sol–gel, hydrothermal, combustion, thermolysis, microwave-assisted synthesis, core@shell synthesis techniques, etc. have been described. Chapters 3 and 4, authored by Jain et al.; Ojha and Ojha, refer to characterization techniques and analysis; Raman and FTIR spectroscopic techniques and their applications, respectively. Various structural and optical techniques for the characterization of UCNPs, viz. X-ray diffraction (XRD), X-ray photoelectron spectroscopy (XPS), field emission scanning electron microscopy (FESEM), transmission electron microscopy (TEM), energy-dispersive X-ray spectroscopy (EDS), thermogravimetric analysis (TGA), ultraviolet–visible–near infrared (UV–Vis–NIR) absorption spectroscopy, dynamic light scattering (DLS), photoluminescence, Fourier transform infrared (FTIR), have been reported. Chapters 5, 6 and 7, authored by Ranjan et al.; Prasad and Rai; and Pattnaik and Rai, summarize the fundamental aspects of UCNPs based on their properties, frequency upconversion in UCNPs containing transition metal ions, and frequency upconversion in UCNPs containing rare-earth ions, respectively . Along with introduction the dynamics of UCNPs on the basis of fluorescence decay times, quantum yield measurement of UCNPs, frequency upconversion and its various mechanisms have also been interpreted. The various routes to enhance the upconversion luminescence along with the technological applications of UCNPs have been described.

Chapters 8, 9, and 10, authored by Singh; Dwivedi; and Ningthoujam et al., are devoted to the smart and new type of upconverting nanoparticles; surface modification and (bio) functionalization of upconverting nanoparticles, and frequency upconversion in core@shell nanoparticles, respectively. These chapters outline the upconverting core@shell nanostructures, hybrid upconverting nanoparticles, magnetic-upconverting nanoparticles, UC-based metal–organic frameworks, surface modification, bio-functionalization of upconverting materials, synthesis of core@shell and core@shell@shell UCNPs, and use of UCNPs for security, biological, and sensing applications. Chapters 11, 12, 13, 14, and 15, authored by Kumar, Mishra and Shwetabh; Singh et al.; Dey; Mahata, De and Lee; and Shahi and Rai, deal with the UCNPs in solar, forensic, security ink, and anti-counterfeiting applications; application of upconversion in photocatalysis and photodetectors; UCNPs in lighting and displays; upconversion nanoparticles in pH-sensing applications and upconversion nanoparticles in temperature-sensing and optical heating applications, respectively. Chapters 16, authored by Wang et al., throws the light on UCNPs applications in degradation of organic and inorganic pollutants along with the photocatalytic hydrogen generation. The visual detection of fungicides and plant viruses along with the future challenges have been explained by Kesarwani and

Rai in Chapter 17. Chapter 18, authored by Mukherjee and Sahu, involves the application of UCNPs in bio-imaging, drug delivery, photodynamic therapy, and photothermal therapy.

The present book is outcome of the untiring efforts of all the contributing authors. It will be very much helpful to the researchers as well as the undergraduate and post-graduate students studying physics, chemistry, materials science, biology, engineering, etc. in gaining a proper understanding about the upconversion luminescence. It was possible to complete this book only due to the great affection and blessings of Gurudev Pt. Shri Ram Sharma Acharya and Gurumataji Mata Bhagawati Devi Sharma. Special thanks to all my family members and research scholars for their motivation and kind support. I would also like to thank the Wiley team involved from the beginning till the completion of the book proposal. As a large number of topics related to the UCNPs and their applications have been covered in this book, there could be the possibility that some of the minute glitches have been missed out. Therefore, genuine suggestions and comments from the readers are welcome. Overall, the research developments on UCNPs and their uses in different fields starting from very basics to advanced level make the present book unique.

Department of Physics
Indian Institute of Technology
(Indian School of Mines),
Dhanbad, India

*Professor (Dr.) Vineet K. Rai*

# 1

# Introduction to Upconversion and Upconverting Nanoparticles

*Manisha Mondal*[1,2] *and Vineet Kumar Rai*[1]

[1] *Indian Institute of Technology (Indian School of Mines), Department of Physics, Laser and Spectroscopy Laboratory, Dhanbad 826004, Jharkhand, India*
[2] *Tezpur University (Central University), Department of Physics, Napaam, Tezpur, Sonitpur 784028, Assam, India*

## 1.1 Introduction

Spectroscopy almost deals with the interaction of light and matter. It provides information about splitting of electromagnetic radiation into its constituent wavelengths. The beginning of spectroscopy lies since the observation of light dispersion through prism by Sir Isaac Newton. Among different spectroscopy techniques, optical spectroscopy delivers an exceptional tool by which one can find detailed information regarding the absorbing and emitting atoms, ions, molecules, defects, their local surroundings, etc. In a term, optical spectroscopy allows light to penetrate inside materials. Optical spectroscopy can be characterized into four parts: absorption, luminescence, reflection, and scattering. A marvelous dimension of research carried out in finding novel luminescent materials plays an important role in optical communication, lighting, medical diagnosis, etc. (Berthou and Jörgensen 1990; Cheng et al. 2013; Jiang et al. 2016; Lin et al. 2016; You et al. 2016; Dey and Rai 2017; Mehra et al. 2020). When an atomic system after absorbing the photons of appropriate frequency transits upward to a higher state and then by the spontaneous emission process, it may return to the ground state. This de-excitation route is familiar as the luminescence process. The occurrence of luminescence due to excitation of light is known as photoluminescence. On the other hand, luminescence due to excitation of an electron beam is termed as cathodoluminescence, which helps to identify impurities, lattice defects, and crystal distortions. Radioluminescence occurs due to excitation through the highly energetic electromagnetic radiations (i.e. $\alpha$ rays, $\beta$ rays, and $\gamma$ rays). The thermoluminescence phenomena are used in radiation dosimetry, dating of minerals and old ceramics, materials characterization, biology, forensic, etc. It occurs when a material radiates light as a consequence of release of energy kept in traps by thermal heating. Electroluminescence occurs due to the passage of electric current over a material. The emission of light due to mechanical disturbance originates triboluminescence. Conferring to the diverse positions of

*Upconverting Nanoparticles: From Fundamentals to Applications*, First Edition. Edited by Vineet K. Rai.

the excitation and emission bands, the luminescent materials can be categorized into Stokes- and anti-Stokes-type luminescent materials. These processes are typically exemplified by the Jablonski diagram (Jablonski 1935; Jablonski 1993). The luminescent materials are commonly known as phosphors, which means "light bearer," that consist of host and dopants. In these constituents, lanthanide materials are mainly introduced into the host matrix. Lanthanides have the most complicated electronic structures because of their large number of incomplete 4f energy levels. The present chapter presents a brief outlook on understanding the frequency conversion mechanisms, electronic energy levels of rare-earth (RE) ions, transition metal ions, theoretical description of the optical characteristics of RE ions, and Upconverting nanoparticles (UCNPs).

## 1.2 Frequency Conversion and Its Various Processes

The photoluminescent materials are able to display visible emissions via suitable ultraviolet (UV) or near-infrared (NIR) excitations. In the majority of cases, excitation energy is greater than emitted photon energy; this emission is called as Stokes emission, and the corresponding energy loss is known as Stokes shift. In certain circumstances, emitted energy is higher than absorbed energy; this is known as anti-Stokes emission.

### 1.2.1 Stokes Emission

The Stokes-type emission process possesses two types of features such as downconversion and quantum cutting (Huang et al. 2013; Loo et al. 2019). In quantum cutting process, two or more lower energy photons are emitted for each incident high-energy photon absorption. In this process, two, three or four low-energy photons are emitted because of the absorption of one NIR, visible, or ultraviolet photon. In this process, the conversion efficiency is more than 100%. In current years, quantum cutting has acknowledged considerable devotion as a budding method to improve the photovoltaic conversion efficiency of solar cells. On the other hand, in the downconversion process, emission of one lower energy photon takes place because of the absorption of one higher energy photon; thus, the conversion efficiency will not go beyond 100%.

### 1.2.2 Anti-Stokes Emission

The anti-Stokes emission process occur via three processes: two-photon absorption (TPA), second harmonic generation (SHG), and upconversion (UC) (Figure 1.1) (Pollnau et al. 2000; Gamelin and Gudel 2000; Suijver 2008; Grzybowski and Pietrzak 2013; Chen et al. 2015; Nadort et al. 2016). TPA is a type of nonlinear absorption process that can be defined as the simultaneous absorption of two photons of same or different frequencies by an atom, ion, or molecule. In this process, the electron is promoted from low energy level (i.e. ground state) to excited

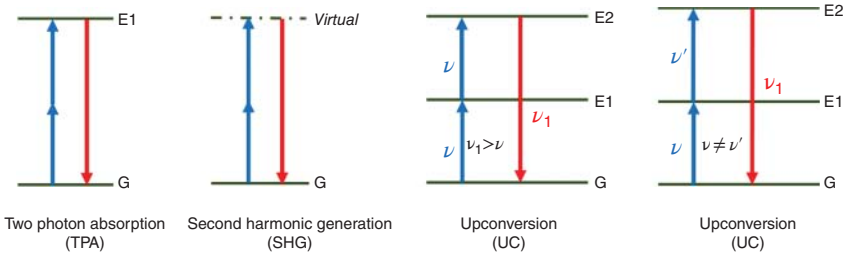


**Figure 1.1** Basic energy-level diagrams depicting typical anti-Stokes processes.

level, and the energy of the emission transition is equal to the sum of two-photon energies. As this is a third-order nonlinear process, it is effective at precise high intensities. TPA was initially anticipated by Maria Goeppert-Mayar in the year 1931. This was experimentally verified by the laser after its discovery. A number of techniques are used to measure TPA, such as two-photon excited fluorescence, z-scan, nonlinear transmission, etc. On the other hand, SHG, "an optical nonlinear process," occurs from a virtual state in a medium having second-order nonlinear susceptibility. This was revealed and experimentally verified by Franken et al. (1961). They detected the second harmonic light when an intense beam of 6943 Å from the ruby laser was passed through the quartz crystal. In this process, two photons of the same frequency interact with a nonlinear material (i.e. medium) and give rise to a new photon of double the frequency or energy of the incident photons. Furthermore, UC is also an anti-Stokes process that converts the lower energy photons into high-energy photons, e.g. infrared to visible or UV light (Figure 1.1). It is a stepwise absorption process involving intermediate states (Auzel 1966; Ovsyakin and Feofilov 1966). Basically, among these three processes of converting lower energy photons into higher energy photons, TPA and SHG need a coherent beam as well as a very high excitation beam intensity. In the UC process, coherent pumping and high intensity of the excitation beam are not necessarily required. It occurs even at low intensity of the excitation beam because of the presence of real intermediate states (generally, of metastable nature).

The materials that exhibit the UC properties are known as upconverting materials. In recent years, these upconverting materials are extensively used in sensing, infrared counters, solid-state lasers, solar cells, fingerprint detection, security ink, upconverters, biological fields, etc. (Digonnet 1993; Wade et al. 2003; Rai 2007; Wang and Liu 2009; Gu et al. 2013; Li et al. 2013; Wang and Zhang 2014; Chen et al. 2014; Mondal and Rai 2020). Generally, the UC phenomenon observed in these materials is not as simple as depicted in Figure 1.1. Several processes accountable for UC mechanisms are as follows.

#### 1.2.2.1 Ground/Excited-State Absorption (GSA/ESA)

Ground-state absorption (GSA) is one of the simplest routes for UC mechanism (Auzel 1973, 2004; Garlick 1976; Rai et al. 2013; Reddy et al. 2018). The process in which the ground-state ions (i.e. electrons) after absorbing the requisite energy from the pump photons are promoted to the first intermediate level is known as the GSA

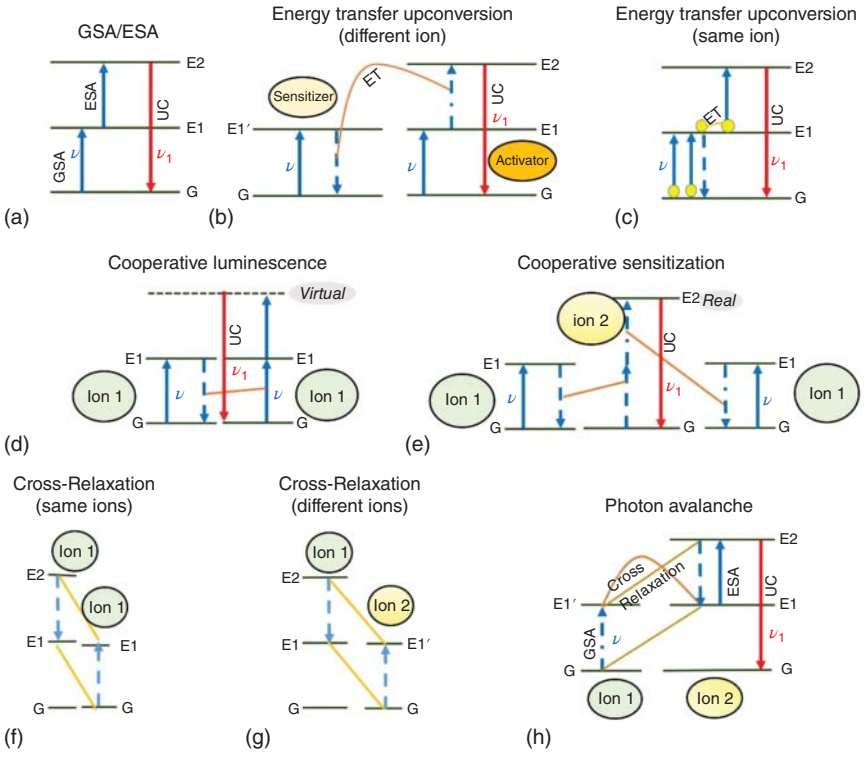


**Figure 1.2** Schematic representation of possible UC mechanisms: (a) GSA/ESA, (b and c) ETU, (d) cooperative luminescence, (e) cooperative sensitization, (f and g) CR, and (h) PA processes.

process. Conversely, sequential absorption of two light quanta by a particular ion is known as ESA process (Auzel 1973, 2004; Garlick 1976; Rai et al. 2013). In the case of ESA process, the ion present in the intermediate state absorbs the second photon and transits upward to the next higher state. For example, the energy-level diagrams for GSA and ESA mechanisms are presented in Figure 1.2a. Here at first, an ion absorbs the pump photon of energy (=$h\nu$, where "$h$" is Planck's constant and "$\nu$" is the frequency of the incident photon) and reaches to the intermediate state E1 (exhibit long lifetime) from the ground state G via the GSA process and then a second pump photon (of the same energy) excites the ion from E1 state to the next higher state E2. A radiative decay of the ion from the excited state (E2) to the ground state (G) results in UC emission. Thus, a single ion is involved in the whole ESA process. For getting proficient UC emission through the ESA process, a ladder-like energy-level arrangement in ions is essential.

#### 1.2.2.2 Energy Transfer Upconversion (ETU)

Like the ESA process, the energy transfer upconversion (ETU) process also involves successive absorption of two energy quanta by the ions to occupy the intermediate (i.e. metastable) state (Figure 1.2). As in the ESA process there is an involvement

of single ion, however, ETU operates within two (similar or different) ions. In this mechanism, the involved two dopant ions are termed as sensitizer and activator (Heer et al. 2003; Boyer et al. 2007; Shan et al. 2007; Soni et al. 2015; Mukhopadhyay and Rai 2020; Pattnaik and Rai 2020). At first, both the (different) ions absorb the pump photons from the ground state and then moves to their respective metastable states ($E1'$ and E1, where $E1' \cong E1$) through the GSA process (Figure 1.2b). After that, the sensitizer ion (present in $E1'$ state) handovers its excitation energy to the neighboring activator ion (present in E1 state) and relaxes back to the ground state. The activator ion after gaining this excitation energy from the sensitizer reaches to the next higher energy state (E2).

When the two involved dopant ions are similar, these two ions are initially excited to the intermediate state (E1) after receiving the energy from pump photons (Figure 1.2c). The two ions present in the E1 state exchange their energy in such a way that one ion (i.e. donor), after transferring its excitation energy to the other excited ion (i.e. acceptor), decays nonradiatively to the lower energy level (G). The other ion (i.e. acceptor) after getting excitation energy from the first one (i.e. donor) is promoted to the next higher energy state (E2). A radiative transition from state E2 to the ground state (G) generates a photon of energy ($=h\nu_1$), which is higher than the incident photon energy ($=h\nu$) (Figure 1.2). This ETU process is the most efficient UC emission process (Auzel 2004; Rai et al. 2007, 2008). In this process, the dopant ion concentration (which regulates the average distance concerning adjacent dopant ions) plays a key role in the UC emission intensity.

#### 1.2.2.3 Cooperative Luminescence and Cooperative Sensitization Upconversion (CSU)

UC emission by a cooperative energy transfer process involves two ions (one acts as a donor and the other ion as an acceptor). In the cooperative luminescence process, two ions absorb the pump photons successively and reach the higher (intermediate) state E1 (Figure 1.2d). In this intermediate level, these two ions transfer their energy in such a way that one ion (donor) transfers its excitation energy to the other one (acceptor) and the donor returns to the ground state (G). The acceptor, after gaining the excitation energy from the donor, transits upward to a higher energy state, "which is a virtual state." This virtual state is also known as the cooperative energy state (Lee et al. 1984; Maciel et al. 2000; Diaz-Torres et al. 2005). From this virtual state, it relaxes radiatively to the ground state (G) via emitting a photon of energy larger than the incident photon energy (Figure 1.2d). On the other hand, in the cooperative sensitization process, when the energy of the two excited ions are transferred to a third ion (ion 2), then it goes from the ground state to an excited state having energy equal to the sum of the energies of the two individual ions (Martín et al. 2001; Salley et al. 2001, 2003). In Figure 1.2e, the excitation energy of the two excited ions (ion 1) present in the state E1 is transferred to a third ion (ion 2). The third ion (ion 2) present in the ground state (G), after absorbing the excitation energy corresponding to the two excited ions (ion 1), moves to its higher state (E2). After that, the third ion from the excited state (E2) relaxes radiatively to the lower levels (say ground state) via emitting the photons of energy higher than that of

the incident photon. This process is known as cooperative sensitization, and the emitting state (E2) in this process is a real state (Figure 1.2e). Thus, the cooperative sensitization is more effective than cooperative luminescence because it may compensate the low UC emission efficiency (Dwivedi et al. 2007; Liang et al. 2009).

#### 1.2.2.4 Cross-relaxation (CR) and Photon Avalanche (PA)

The cross-relaxation (CR) process occurs due to ion–ion interaction (ions may be similar or different) (Chen et al. 2014; Pattnaik and Rai 2020) (Figure 1.2f,g. The cross-relaxation between two identical ions/molecules is responsible for self-quenching (Figure 1.2f). In the self-quenching process, the intermediate states of both the ions (ion 1) have the same energy (E1). When the cross-relaxation occurs between two different ions (Figure 1.2g), the first ion shares a part of its excitation energy to the second ion by the process E2 (ion 1) + G (ion 2) → E1 (ion 1) + E1′ (ion 2) (Figure 1.2g). In this process, the first ion (ion 1) initially present in the excited state (E2) interchanges a part of its excitation energy to the second ion (ion 2) that is initially available in the ground state (G). By this way, the decrease in the energy of the first ion (ion 1) is equal to the increase in the energy of the second ion. This results in both the ions/molecules changing simultaneously to the excited state (E1 and E1′). Among the other UC processes, the most exciting process is photon avalanche (PA), which was first experimentally observed in $Pr^{3+}$-doped infrared quantum counters (Chivian et al. 1979). Generally, this PA process occurs when the excitation energy exceeds its threshold limit. When the excitation energy is lower than the threshold energy, the emitted intensity is very poor, but as it exceeds the limit, the emitted intensity becomes enormously greater (Joubert 1999; Singh et al. 2011; Zhu et al. 2012; Mondal et al. 2016). For occurrence of PA process, at first, the intermediate level and the upper excited level are populated by the GSA, ESA, and ETU processes. By the CR process between these upper excited level and the ground state of a neighboring ion, two ions are generated in the intermediate level E1 (Figure 1.2h). Now, two ions are available in the intermediate state for the ESA process. Thus, with the feedback looping of ESA and CR processes simultaneously, the number of ions in the intermediate level increases, which give rise to strong UC emission.

The PA process is an unusual pumping process because it may lead to strong UC emission from the upper excited state E2 without any resonant GSA from the ground state (G) to the intermediate state (E1) of ion 2 (Figure 1.2h). The frequency of incident photon is in resonant with state E1′ of ion 1 and the upper excited state E2 of ion 2. An efficient CR process, i.e. E2 (ion 2) + G (ion 1) → E1 (ion 2) + E1 (ion 1), occurs between ion 1 and ion 2. This results in both the ions to occupy the intermediate state E1. These two ions readily populate the level E2 through ESA to further initiate the cross-relaxation. With the feedback looping of these efficient cross-relaxation and ESA processes, the number of ions in the intermediate state E1 increases rapidly, which results further an enormous increase in the population of level E2. Thus, in the PA process, a strong UC emission from state E2 to the ground state G (of ion 2) has been observed.

## 1.3 Transition Metals and Their Properties

The optical centers are necessary for the perfect crystals to exhibit the optical spectra. Depending on the absorption and emission bands of the optical centers present in the pure crystals, they are pertinent for diverse applications, such as optical amplifiers, solid-state lasers, color displays, absorbers, improving in luminescence brightness, fibers, optical switches, etc. Any element in the periodic table may act as a foreign element in the crystal. However, essentially, a few number of elements can be ionized, which can generate energy levels and thus yield optical features. For industrial applications, the two extremely important elements are transition metals and REs in the periodic table. Transition metal ions are especially used as optically active dopants in tunable solid-state lasers (Solé et al. 2005). These ions belong to the fourth period of the periodic table with electronic configuration $1s^2 2s^2 2p^6 3s^2 3p^6 3d^n$, where "$n$ (varies from 1 to 10)" is the number of 3d electrons present in the transition metal ions. Generally, valence electrons are responsible for optical transitions; hence, in the case of transition metals, 3d electrons are accountable. Because of the large radius of transition metal ions as compared to lanthanides and no shielding of valence electrons, strong field effect occurs; hence, they exhibit the broad bands.

The Sugano–Tanabe diagram explains the energy-level diagram for the transition metal ions (Figure 1.3) (Tanabe and Sugano 1954a,b). The spectroscopic terms for the free ion states of the transition metal ions due to the L-S interaction are described

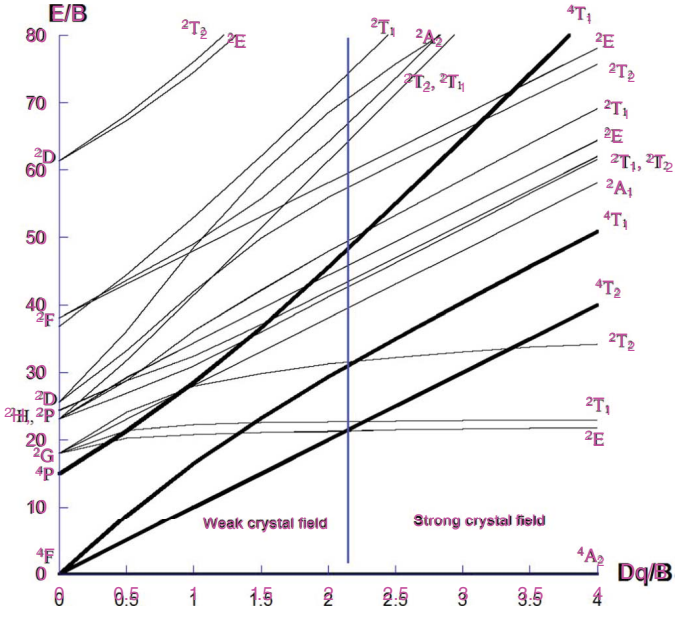


**Figure 1.3** Tanabe–Sugano diagram for the $d^3$ electron configuration in the octahedral crystal field. Source: Brik et al. (2016). Reprinted with permission of The Electrochemical Society.

as ${}^{2S+1}L_J$, where, $L$, $S$, and $J$ denote the total orbital angular momentum, total spin angular momentum, and total angular momentum, respectively. The energy separation among the ${}^{2S+1}L$ states, i.e. the strength of the electron–electron interaction, can be calculated with the help of Racah parameters (A, B, and C) (Solé et al. 2005). On the basis of octahedral crystal lattice, Sugano and Tanabe explained the occurrence of energy levels in the case of transition metal ions, but by using this diagram, one can also interpret the optical spectra arising from the transition metal ions in different types of host lattices.

This diagram explains the splitting of ${}^{2S+1}L$ free ion energy states with the ratio between the strength of the crystal field and the electron–electron interaction strength (symbolized as Dq/B) versus the free ion energy levels (E/B units). In this diagram, the *y*-axis is in terms of energy "E" scaled by B (one of the Racah parameters). The splitted terms for ${}^{2S+1}L$ energy states are termed as A, T, and E levels. This Sugano–Tanabe diagram also explains the nature of the optical bands for transition metal ions. In the case of strong crystal field approximation, the crystal field effect dominates over the electron–electron interaction among 3d ions. Accordingly, there are three single-electron orbitals for each orbital. Furthermore, according to the Sugano–Tanabe diagram, for low crystal field strength, the emission band is shifted toward the lower energy side. For this specific nature, the emission wavelength in the transition metal ions depends on a particular host material. Thus, doping of transition metal ions in different host materials directed to the advancement of countless varieties of tunable solid-state lasers. Most of the transition metal ions are incorporated in the octahedral crystal host matrix, so their energy level can be explained on the basis of Sugano–Tanabe diagram (Tanabe and Sugano 1956). However, in some cases, such as $Ni^{2+}$, $Co^{2+}$, and $Cr^{2+}$ ions, these transition metal ions are incorporated in the tetrahedral crystal lattice for different applications; therefore, the Konig and Kremer diagram (Konig and Kremer 1997) is applicable in explaining the energy levels of transition metal ions other than the octahedral one.

## 1.4 Rare Earths and Their Properties

Most of the lasers, phosphors, amplifiers, etc., comprise RE elements. Surprisingly, the global applications of RE-based materials are increasing from industry applications to medical applications. There are 15 lanthanide elements along with two more elements i.e. scandium (Sc) and yttrium (Y). These 15 lanthanide elements are commonly named as lanthanum (La), cerium (Ce), praseodymium (Pr), neodymium (Nd), promethium (Pm), samarium (Sm), europium (Eu), gadolinium (Gd), terbium (Tb), dysprosium (Dy), holmium (Ho), erbium (Er), thulium (Tm), ytterbium (Yb), and lutetium (Lu). Most of the RE elements are entitled as per the name of the inventors or the name of their revealed places. These RE elements are incorporated in different host materials in their ionized (either divalent or trivalent) form. The divalent RE ions {Eu (+2), Yb (+2), and Sm (+2)} possess one more electron compared to the trivalent ions and thus exhibit different optical features and treat differently.

### 1.4.1 Trivalent Rare-Earth Ions

The outer most electronic configurations of divalent and trivalent RE ions are 5d $4f^n$ $5s^2$ $5p^6$ and $4f^n$ $5s^2 5p^6$, respectively, where $n$ (varies from $n = 0$ to 14) specifies the number of electrons in the unfilled 4f shell. These $4f^n$ electrons are the valence electrons that are accountable for the spectroscopic transitions.

#### 1.4.1.1 Electronic Structure

The presence of valence electrons in the 4f shell makes the RE ions as luminescent centers of any phosphor material. The group of 15 elements comprising atomic number starting from 57 to 71 in the sixth period of the periodic table together with scandium (Sc) and yttrium (Y) are known as RE elements. When these RE elements are introduced into the hosts, they easily convert into their either doubly or triply ionized states to acquire their stable electronic configurations. The outer most electronic configurations of lanthanum (La, atomic number Z = 57) and the last element lutetium (Lu, Z = 71) in their triply ionized state are $4f^0$ $5s^2$ $5p^6$ and $4f^{14}$ $5s^2$ $5p^6$, respectively. There are fifteen possibilities for filling these 4f orbitals as the f orbital contains seven suborbitals. Actually, these unfilled 4f valence electrons are in control for optical transitions. Table 1.1 presents the electronic arrangements and ground states of each triply ionized RE element. The actual electronic configuration of the 15 RE elements (i.e. from La to Lu) is [Xe] $5d^1$ $6s^2 4f^n$ ($n = 0$ to 14). However, in

**Table 1.1** Electronic configuration of trivalent ionic states of RE elements (Shionoya et al. 1998).

| Ion | Atomic number | Number of 4f electrons ($n$) and electronic configuration | $S = \Sigma s$ | $L = \Sigma l$ | $J = L - S$ ($n < 7$) $J = L + S$ ($n \geq 7$) | Ground state |
|---|---|---|---|---|---|---|
| $La^{3+}$ | 57 | 0 and [Xe]$4f^0$ | 0 | 0 | 0 | $^1S_0$ |
| $Ce^{3+}$ | 58 | 1 and [Xe]$4f^1$ | 1/2 | 3 | 5/2 | $^2F_{5/2}$ |
| $Pr^{3+}$ | 59 | 2 and [Xe]$4f^2$ | 1 | 5 | 4 | $^3H_4$ |
| $Nd^{3+}$ | 60 | 3 and [Xe]$4f^3$ | 3/2 | 6 | 9/2 | $^4I_{9/2}$ |
| $Pm^{3+}$ | 61 | 4 and [Xe]$4f^4$ | 2 | 6 | 4 | $^5I_4$ |
| $Sm^{3+}$ | 62 | 5 and [Xe]$4f^5$ | 5/2 | 5 | 5/2 | $^6H_{5/2}$ |
| $Eu^{3+}$ | 63 | 6 and [Xe]$4f^6$ | 3 | 3 | 0 | $^7F_0$ |
| $Gd^{3+}$ | 64 | 7 and [Xe]$4f^7$ | 7/2 | 0 | 7/2 | $^8S_{7/2}$ |
| $Tb^{3+}$ | 65 | 8 and [Xe]$4f^8$ | 3 | 3 | 6 | $^7F_6$ |
| $Dy^{3+}$ | 66 | 9 and [Xe]$4f^9$ | 5/2 | 5 | 15/2 | $^6H_{15/2}$ |
| $Ho^{3+}$ | 67 | 10 and [Xe]$4f^{10}$ | 2 | 6 | 8 | $^5I_8$ |
| $Er^{3+}$ | 68 | 11 and [Xe]$4f^{11}$ | 3/2 | 6 | 15/2 | $^4I_{15/2}$ |
| $Tm^{3+}$ | 69 | 12 and [Xe]$4f^{12}$ | 1 | 5 | 6 | $^3H_6$ |
| $Yb^{3+}$ | 70 | 13 and [Xe]$4f^{13}$ | 1/2 | 3 | 7/2 | $^2F_{7/2}$ |
| $Lu^{3+}$ | 71 | 14 and [Xe]$4f^{14}$ | 0 | 0 | 0 | $^1S_0$ |

the triply ionized state, these elements lose their 5d and 6s orbital electrons; hence, the outer most electronic configuration of trivalent RE ions becomes $4f^n\ 5s^2 5p^6$ (Table 1.1). Therefore, due to the larger radii of 5s and 5p orbitals compared to the 4f orbital, these 4f electrons are shielded by 5s and 5p orbitals. Unlike transition metals when doped into solid materials, the outer 3d electrons are strongly affected by the crystal field effect; in the case of RE ions due to this shielding effect when they are incorporated into a solid host, the 4f electrons are weakly perturbed. Because of this shielding of 4f electrons by the completely filled outer electronic shells ($5s^2\ 5p^6$), the relative positions of 4f energy levels in the RE ions do not vary very much from one host to the other. Owing to this exceptional property of the triply ionized RE ions, they exhibit sharp absorption and emission spectra and thus have longer lifetime.

#### 1.4.1.2 Interaction of Rare-Earth Ions

The 4f–4f transitions are parity forbidden according to the Laporte selection rule, but when incorporated into a host matrix, the electronic structure of the REs are perturbed, and because of the intermixing of $4f^n$ and $4f^{n-1}$ 5d orbitals, the optical transitions become allowed. Because of this intermixing, the parity of levels is changed and the transitions become allowed. These transitions are known as electric dipole allowed transitions. By using Schrodinger's equation, the energy levels of the RE ions responsible in optical transitions can be calculated as (Auzel 2004; Solé et al. 2005)

$$H\Psi = E\Psi \tag{1.1}$$

where "Ψ" is the eigenfunctions of the optical center and "$H$" denotes the Hamiltonian because of the diverse interactions of the 4f orbital electrons. Generally, the crystal field theory and the molecular orbital theory (MOT) have been used to describe the interaction between the RE elements and the host matrices.

***Crystal Field Theory*** The crystal field theory was first described by Hans Bethe and John Hasbrouck van Vleck in the year 1930. In the case of transition metal ions when incorporated in a host material, the outer electrons are greatly affected by the surrounding host environment. However, in the case of RE ions when doped into a host material, the energy levels are only slightly perturbed because of the shielding by the $5s^2\ 5p^6$ orbitals. This breaking of degeneracy of the d and f electron orbitals can be described on the basis of crystal field theory (Wybourne 1965; Wybourne and Meggers 1965; Carnall et al. 1989; Auzel 2004; Liu 2005, 2015; Solé et al. 2005). The filled orbitals in the case of RE ions are 4d, 5s, and 5p, whereas 4f, 5d, and 6s are valence electron shells in their triply ionized state. Because of the larger radii of 5s and 5p orbitals, the 4f electrons of the RE ions are protected from the surrounding perturbation. The energy levels of the RE elements can be represented by some elementary quantum mechanical terms, total orbital angular momentum $L$ (sum of total quantum number $l$), total spin angular momentum $S$ (sum of total quantum number $s$), and the total angular momentum $J$ ($=L+S$). With the help of Schrodinger's equation, the interaction between the RE ions and the host element